Biomarkers, 2012; 17(2): 125–133

ISSN 1354-750X print/ISSN 1366-5804 online
DOI: 10.3109/1354750X.2011.643485

informa
healthcare

RESEARCH ARTICLE

Identification and quantification of osteopontin splice variants in the plasma of lung cancer patients using immunoaffinity capture and targeted mass spectrometry

Jiang Wu[1], Pooja Pungaliya[1], Eugenia Kraynov[2], and Brian Bates[1]

[1]*Global Biotherapeutic Technologies and* [2]*Pharmacokinetic, Dynamics, and Metabolism, Pfizer Worldwide Research and Development, Groton, CT, USA*

Abstract

The expression patterns and functional roles of three osteopontin splice variants (OPNa, b, and c) in cancer metastasis and progression are not well understood due to the lack of reliable assays to differentiate the isoforms. We have developed a mass spectrometric method to quantify OPN isoforms in human plasma. The method is based on the immunocapture of all OPN isoforms, followed by MRM–MS analysis of isoform-specific tryptic peptides. We were able to simultaneously identify and quantify all three isoforms in the plasma of 10 healthy individuals and 10 non-small cell lung cancer (NSCLC) patients. Our results show that none of the OPN splice variants is cancer specific. However, OPNa, the major isoform in healthy and NSCLC plasma, is substantially elevated in NSCLC patients, whereas OPNb and OPNc are at equivalent levels in two populations.

Keywords: Osteopontin, splice variant, NSCLC, plasma, MRM–MS

Introduction

Osteopontin (OPN) is a highly acidic phosphorylated glycoprotein secreted by a variety of cells and present in most tissues and body fluids. It is implicated in a variety of physiological processes such as bone mineralization, inflammation, and tumor growth (Courter et al. 2010, Jain et al. 2007, Kazanecki et al. 2007, Rangaswami et al. 2006, Wai & Kuo 2008). In many tissues, OPN functions to promote cell adhesion and to facilitate cell migration or survival through its interaction with integrins and CD44 variants (Banerjee et al. 2008, Christensen et al. 2007, Courter et al. 2010, Rangaswami et al. 2006, Wai & Kuo 2008, Weber et al. 2002). In cancer, OPN has been shown to regulate multiple tumor promoting mechanisms including cell proliferation, survival, adhesion, migration, invasion and angiogenesis (Allan et al. 2006, Blasberg et al. 2010a, Courter et al. 2010, Creaney et al. 2011, Ivanov et al. 2009, Jain et al. 2007, Mi et al. 2004, Rangaswami et al. 2006, Wai & Kuo 2008, Weber et al. 2002).

The functional diversity of OPN is partly attributable to the presence of multiple molecular forms resulting from extensive post-translational modifications such as phosphorylation, glycosylation, sulfation, and proteolytic processing, causing differential binding of OPN to various types of integrins and CD44 variants (Blasberg et al. 2010a, Christensen et al. 2007, Christensen et al. 2005, Christensen et al. 2008, Kazanecki et al. 2007, Keykhosravani et al. 2005, Weber et al. 2002). Another underlying mechanism accounting for functional complexity of OPN is alternative RNA splicing. Three splice variants (OPNa, OPNb and OPNc) are found in human, with OPNb and OPNc lacking exon 5 and exon 4 in the N-terminal portion of the OPN respectively (Blasberg et al. 2010a, Chae et al. 2009, Goparaju et al. 2010, He et al. 2006, Ivanov et al. 2009, Mirza et al. 2008, Paleari et al. 2009, Sullivan et al. 2009) (Figure 1).

The role of OPN in regulating cancer progression has been the subject of intense investigation. Elevated OPN levels in plasma and tissues are strongly correlated with

Address for Correspondence: Dr. Jiang Wu, Structural Biology and Biophysics, Pfizer Worldwide Research and Development, Eastern Point Road, Groton, CT 06340, USA. Tel: (860)441-1169. Fax: (860)715-9688. E-mail: jiang.wu@pfizer.com; brian.bates11@gmail.com

(Received 10 October 2011; revised 16 November 2011; accepted 20 November 2011)

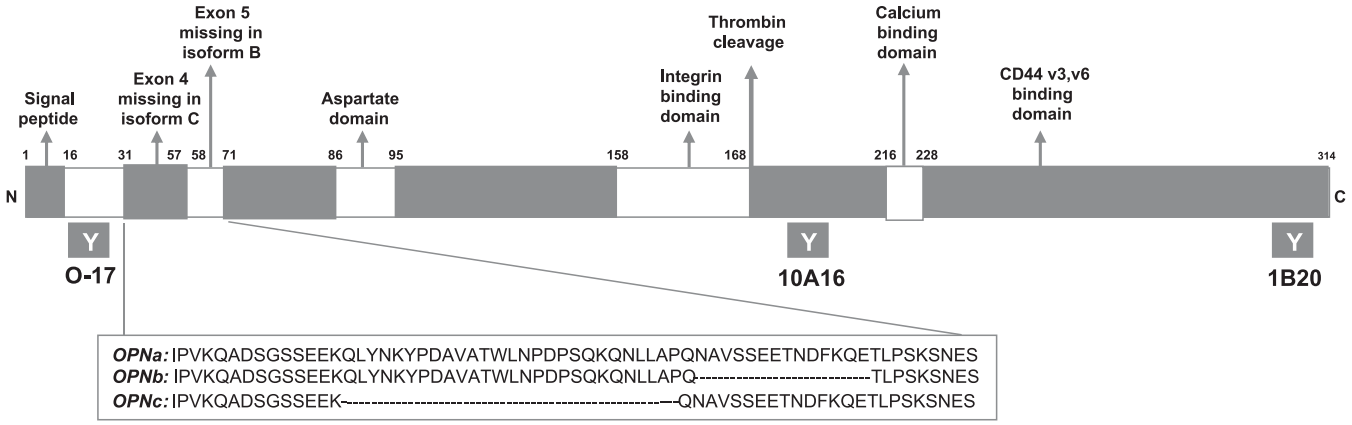

Figure 1. Schematic representation of the domain structure of osteopontin (OPN). The structure of OPN can be divided into multiple domains that are highly post-translationally modified. Expanded inset in green shows protein sequence for OPNa, b, and c around the exon 3–6 junction. Note the absence of exon 4 sequence in OPNc and exon 5 in OPNb. Antibody binding regions are indicated.

disease progression and poor survival in many different human cancers, suggesting an important but poorly understood role for this protein in tumorigenesis and metastasis. A number of studies suggest that the plasma concentration of OPN is significantly elevated in early-stage NSCLC. The levels are reduced after resection and appear to increase with recurrence (Blasberg et al. 2010b, Creaney et al. 2011). Mack et al (Mack et al. 2008) observed that lower OPN plasma levels are associated with superior outcomes in advanced non-small-cell lung cancer patients receiving platinum-based chemotherapy. It is likely that OPN can serve as a potential prognostic marker of cancer progression (Allan et al. 2006, Anborgh et al. 2009, Blasberg et al. 2010a, Blasberg et al. 2010b, Chae et al. 2009, Chang et al. 2007, Goparaju et al. 2010, He et al. 2006, Ivanov et al. 2009, Mack et al. 2008, Mi et al. 2004, Mirza et al. 2008, Nicol et al. 2008, Plumer et al. 2008, Sullivan et al. 2009, Zhao et al. 2011).

However, the functional specificity and relative expression of individual OPN isoforms in human tumors are not well characterized. Using isoform-specific RT-PCR, Jain et al found that OPNa and OPNb but not OPNc were the main isoforms overexpressed in soft tissue sarcomas (STS), (NSCLC), and head and neck squamous cell carcinomas (HNSCC) (Jain et al. 2007). On the other hand, Mirza et al reported that OPNc is selectively expressed in invasive breast tumor cell lines (Mirza et al. 2008). They reported that while OPNa and b were found in both normal and disease samples the mRNA for OPNc was preferentially found in breast cancers specimens (Mirza et al. 2008). Interestingly, siRNA-mediated knock-down of OPN inhibits lung cancer cell proliferation, invasiveness and *in vivo* tumor growth (Zhao et al. 2011). In this study, the proliferation of the tumor cells was linked to OPNb while invasiveness was correlated with OPNc expression. Goparaju et al reported the similar observation that OPN isoforms play different roles in determining the metastatic potential of NSCLC (Goparaju et al. 2010). OPNa expression was increased in 91% of NSCLC tumors they examined compared with matched lung, and its overexpression enhanced activity in proliferation and invasion assays. In contrast, OPNc overexpression considerably decreased proliferation, colony formation, and invasion, whereas OPNb overexpression had more subtle effects.

The validation of OPN as a diagnostic biomarker or a therapeutic target requires a more detailed understanding of the expression and activities of the individual isoforms in cells, tissues, and in circulation. Traditionally, such an issue has been approached through development and use of conventional ELISA assays. However, it is often difficult to develop a robust and reliable ELISA for quantification of a protein like OPN which contains extensive and heterogeneous post-translational modifications (Kiernan et al. 2011). In fact, different ELISA kits for plasma OPN have been reported to yield highly variable and non-comparable values (Anborgh et al. 2009, Plumer et al. 2008, Vordermark et al. 2006). For instance, Anborgh et al. (Anborgh et al. 2009) compared six ELISA assays that used different antibodies and measured OPN in plasma from 66 prostate cancer patients. OPN plasma values varied considerably depending on the assay used, with median values ranging from 112 to 1740 ng/mL. Furthermore, assays that are able to simultaneously differentiate OPN isoforms do not exist at present.

Recently, tremendous progress has been made in the application of mass spectrometry for quantification of plasma proteins by measuring their surrogate peptides originating from proteolytic digestion (Kuhn et al. 2004, Makawita & Diamandis 2010, Meng & Veenstra, 2011). With the introduction of heavy isotope-labeled peptides as internal standards and multiple-reaction monitoring (MRM) for targeted acquisition, tens of plasma proteins can simultaneously be quantified with large dynamic ranges and extremely high specificity. In conjunction with immunoaffinity capture of the target proteins or surrogate peptides, such methods enable detection of low ng/mL concentrations of serum and plasma proteins (Kiernan et al. 2011, Kuhn et al. 2009, Nicol et al. 2008,

Ocana & Neubert 2010). This approach has been widely applied to the validation of potential biomarkers discovered by proteomics techniques.

In an attempt to investigate cancer-specific OPN isoform(s), we developed an immunoaffinity-mass spectrometry based method to simultaneously determine concentration of individual OPN isoforms in human plasma. The approach uses a panel of different OPN antibodies to capture all OPN isoforms followed by quantification of the isoform-specific surrogate peptides by the MRM–MS. This method has been applied to the determination of the OPN isoforms in plasma from healthy and NSCLC subjects.

Materials and methods

Materials

Anti-human OPN antibodies (pAb O-17, mAb 10A16, mAb 1B20) were from IBL (Gunma, Japan). Anti-human OPN antibody (MAB1433), Recombinant Human OPN, human OPN ELISA kit (Quantikine) were from R&D systems (Minneapolis, MN, USA). Purity of the recombinant OPN was >90% by SDS–PAGE. Tosyl-activated magnetic beads, tricine mini-gels, and gel loading buffer were purchased from Invitrogen (Carlsbad, CA, USA). Sequencing grade modified trypsin was from Promega (Madison, WI, USA). Poroszyme Immobilized Trypsin was from Applied Biosystems (Foster City, CA, USA). Stable isotope-labeled peptides with a heavy lysine at C-terminus (+8Da), QNLLAPQNAVSSEETNDFK[$^{13}C_6$, $^{15}N_2$] (OPNa), QNLLAPQTLPSK[$^{13}C_6$,$^{15}N_2$] (OPNb), and QNAVSSEETNDFK[$^{13}C_6$,$^{15}N_2$] (OPNc), and their natural analogues (endogenous form) were synthesized by 21st Century Biochemicals (Marlboro, MA). Synthetic peptides purity was determined to be >97% by the reversed-phase liquid chromatography. Alkaline phosphatase was from New England BioLabs (Ipswich, MA). C18 Stage tip was a product of Proxeon (Thermo Fisher, Waltham, MA). All other chemicals were obtained from Sigma–Aldrich (St. Louis, MO).

A total of 20 plasma samples (from 10 healthy individuals and 10 patients diagnosed as NSCLC) were used in the study. The blood samples were collected in BD Vacutainer tubes coated with K2EDTA at certified medical centers and were tested negative to HIV and HBV. The plasma samples were frozen at –80°C until use. The ethnicity information for the healthy sample donors was not available.

Coupling of antibodies to magnetic beads

Each antibody was coupled to 2.8 μm tosyl-activated magnetic beads equilibrated at a 4:1 antibody to bead volume (μg:μL) ratio in 1 M ammonium sulfate, 100 mM borate pH 9.0, according to manufacturer's instructions. After coupling, the active sites on the beads were blocked with 1% BSA. The beads were washed thoroughly with PBS to remove unbound antibody and stored at 4°C.

RT-PCR of OPN gene expression in MDA-MB-435 cells

RT-PCR experiments were performed as previously described by He et al. (He et al. 2006). Briefly, total RNA (Qiagen, Valencia, CA) was extracted from MDA-MB-435 cells provided by Pfizer Oncology. RT-PCR was performed using the same gene specific primers as described (He et al. 2006). Reaction products were analyzed on Agarose gel and sequence confirmed.

Identification of OPN isoforms in MDA-MB-435 cell conditioned medium

MDA-MB-435 conditioned medium (20 mL) was incubated with 2 mg of pAb O-17 immobilized magnetic beads at 4°C overnight with rotation. The beads were washed three times with PBS-1.0% NP-40. Proteins bound to the beads were eluted using 25 μL of tricine gel loading buffer and subsequently separated by a 10–20%. Tricine mini gel (Invitrogen). Gel slices were cut between 40 and 60 KDa and were digested with 1 μg of trypsin overnight. The heavy peptides were added and the peptide mixture was analyzed by nanoLC-MS/MS on an LTQ-Orbitrap XL mass spectrometer (Thermo Fisher, Waltham, MA, USA), using conditions described elsewhere (Shakey et al. 2010). Peptides were identified by searching against human IPI database.

Immunoprecipitation of OPN from human plasma samples

An aliquot (0.1 mL) of the plasma sample from healthy individuals and NSCLC patients was diluted with 0.3 mL of PBS. Each sample was incubated with a mixture of magnetic beads immobilized with different OPN antibodies (2.0 mg O-17 beads, 0.5 mg 10A16 beads, 0.5 mg 1B20 beads, 0.5 mg MAB1433 beads), and rotary mixed at 4°C overnight. The beads were isolated from the unbound material using a magnet, and were sequentially washed three times with 150 μL of PBS-1.0%NP-40, and twice with 150 μL of 10 mM phosphate buffer, pH 7.2. The captured proteins were eluted with 2 × 25 μL of 15 mM HCl. The pH of the solution was neutralized by adding 4 μL of 2 M ammonium bicarbonate solution, and the solution was boiled for 5 min to denature proteins.

An aliquot of standard mixture of heavy isotope-labeled OPN peptides (OPNa 25 fmol, OPNb 12.5 fmol, and OPNc 1.5 fmol) was added to each sample. Proteins were digested with 2.5 μL of immobilized trypsin with vortex overnight at room temperature. After discarding trypsin, the peptides were mixed with 4 μL of 10× NEBuffer3 and 1 μL of alkaline phosphatase. Dephosphorylation was carried out by incubation for 3 hours at 37°C. The resulting sample was desalted using a C18 Stage tip, concentrated in a Speedvac, and stored at –80°C until analyzed by LC–MRM–MS.

LC–MRM–MS analysis

The peptide samples were reconstituted in 75 μL of 0.1% formic acid-5% acetonitrile. An aliquot of 10 μL of each sample was loaded onto a Pico–frit column (New

Objective, Woburn, MA) packed with reversed-phase Magic C18 material (5 μm, 200 Å, 75 μm × 10 cm) and coupled to an LTQ XP mass spectrometer (Thermo Fisher, Waltham, MA). Peptides were separated at a flow rate of 0.2 μL/min using an acetonitrile gradient in 0.1% formic acid of 5%–10% in 7 min, 10%–28% in 23 min, and 28%–90% in 5 min. Electrospray voltage was 1.8 kV. Two MRM transitions were monitored for the doubly charged ion of the native and heavy peptides, respectively (Table 1). The collision energy was set to 35% for all MRM transitions. Each sample was injected and analyzed in triplicate. Peak areas of co-eluting endogenous peptide and the internal standard were determined from the XIC of the two transition ions in the chromatographic separation. The endogenous OPN concentration was calculated by comparing the peak areas of the L/H pairs.

Measurement of plasma OPN concentration by ELISA

The concentration of OPN in the same samples was also measured by the ELISA kit (R&D systems) according to the manufacturer's instructions. The absolute values of the OPN concentration measured by ELISA were compared with the data obtained by the immunoaffinity MRM–MS.

Results

We sought to develop an immunoaffinity-based MRM–MS approach to quantitatively measure the concentration of individual OPN splice isoforms in plasma from healthy and lung cancer subjects. After tryptic digestion, OPNa, b, and c each generated a peptide of unique sequence, which was used as a surrogate peptide for quantification of the respective OPN isoforms. The peptide sequences were subject to a BLAST search (National Center for Biotechnology Information) and confirmed to be specific to the OPN isoforms. The overall strategy is illustrated in Figure 2. Experimentally, OPN was captured from 0.1 mL of the plasma using a mixture of different antibodies recognizing different regions of the OPN sequences. The heavy isotope-labeled peptides were added to the protein mixture as internal standards and the surrogate peptides were generated by digestion using immobilized trypsin. Upon dephosphorylation of the surrogate peptides, the endogenous OPN isoforms were quantified by LC–MRM–MS.

Selection of antibodies for immuprecipitation

OPN is extremely heterogeneous due to mRNA splicing, extensive post-translational modifications and proteolytic truncation. To maximize our ability to capture all OPN isoforms we first screened a variety of anti-human OPN antibodies by IP-Western using MDA-MB-435 breast cancer epithelial cell conditioned medium. Our results demonstrated that the O-17 polyclonal antibody was the most effective commercially available antibody for capturing different OPN isoforms (data not shown). However, to ensure the broadest epitope coverage and minimize bias for or against any particular isoform, we supplemented O-17 pAb pull-down by including three additional antibodies. The final mixture included the aforementioned O-17 pAb which recognizes OPN N-terminal nineteen residues (right after signal peptide), monoclonal antibodies 10A16 and 1B20 that recognize epitopes at the middle and C-terminus of OPN respectively, and MAB1433 that was raised against the whole human OPN sequence and whose exact epitope is unknown.

Method development for surrogate peptide analysis

To develop an assay with the greatest utility we sought to use immune-affinity isolation followed by MRM–MS to

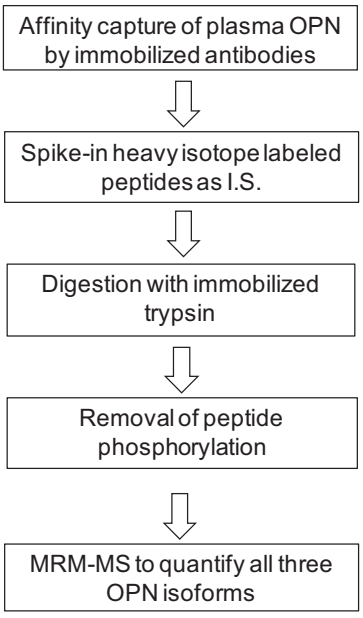

Figure 2. An overview diagram of the immunoaffinity LC–MRM–MS experiment for quantitative measurement of OPN isoforms in plasma.

Table 1. OPN isoform specific peptides and their precursor and transition ions.

OPN isoform	OPN peptide	Precursor ion mass (Da)	Precursor ion charge (z)	Transition ion (m/z)
OPNa	QNLLAPQNAVSSEETNDFK[$^{13}C_6$, $^{15}N_2$]	2112.01	+2	1573.8 (y14), 1644.9 (y15)
	QNLLAPQNAVSSEETNDFK	2104.01	+2	1565.8 (y14), 1636.7 (y15)
OPNb	QNLLAPQTLPSK[$^{13}C_6$, $^{15}N_2$]	1316.75	+2	778.5 (y7), 849.6 (y8)
	QNLLAPQTLPSK	1308.75	+2	770.5 (y7), 841.6 (y8)
OPNc	QNAVSSEETNDFK[$^{13}C_6$, $^{15}N_2$]	1475.66	+2	977.4 (y8), 1064.5 (y9)
	QNAVSSEETNDFK	1467.66	+2	969.4 (y8), 969.4 (y9)

simultaneously detect all three OPN splice variant proteins. Since relative concentrations of the OPN isoforms in plasma is unknown, and OPNb and OPNc recombinant proteins are unavailable, we first used affinity mass spectrometry to determine if it was possible to identify OPN isoforms in a complex sample namely, MDA-MB-435 conditioned medium. Based on RT-PCR analysis (Figure 3) we expect all three splice variants to be produced by this cell line. Immunoaffinity capture using O-17 antibody followed by trypsin digestion and MS identification of the captured proteins identified many OPN peptides common to all three variants (data not shown). In addition, several peptides specific to the OPN variants were unambiguously detected: QNLLAPQNAVSSEETNDFK (OPNa specific peptide), QNLLAPQNAVSpSEETNDFK (OPNa specific phosphopeptide), QNLLAPQNAVSSEETNDFKQETLPSK (OPNa specific peptide with a missed tryptic cleavage), QNLLAPQNAVSpSEETNDFKQETLPSK (OPNa specific phosphopeptide with a missed tryptic cleavage), QNLLAPETLPSK (OPNb specific peptide), and QNAVSSEETNDFK (OPNc specific peptide). The MS and MS/MS spectrum for the OPNc specific peptide and its co-eluting heavy analogue are shown in Figure 4. The same CID fragmentation pattern of the native and heavy peptides confirms the presence of OPNc in the conditioned medium. These data clearly demonstrate that while the isoform-specific peptides were identified with high confidence, some were partially phosphorylated. Furthermore, since solution phase trypsin digestion was incomplete for OPNa (and perhaps OPNc as well since it has the same local sequence) and the N-terminal glutamine of all fragments might be susceptible to conversion to pyroglutamic acid this may diminish the absolute concentration of OPN isoforms measured by this MRM–MS approach.

To address these issues, we next used recombinant OPNa as a tool compound to optimize experimental conditions. We found that immobilized trypsin significantly improved the digestion efficiency, as evidenced by the disappearance of the peptide peak from missed-trypsin cleavage (data not shown). Complete digestion was achieved with 2.5 μL of immobilized trypsin after overnight incubation. Under these conditions, no detectable conversion of glutamine to pyroglutamic acid was observed. Finally, variability due to partial phosphorylation was eliminated by treatment with alkaline phosphatase (data not shown). Therefore, the improved protocol should allow for the unambiguous and quantifiable detection of all OPN splice variants in a complex mixture.

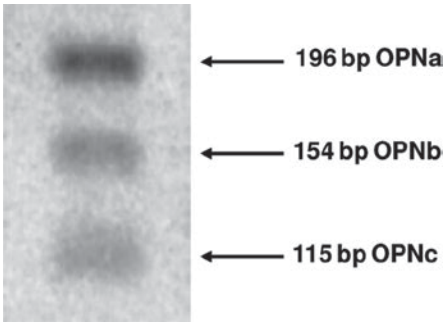

Figure 3. MDA-MB-435 cells express OPNa, b, and c. RT-PCR was performed using isoform-specific primers resulting in isoform-specific bands as indicated. Isoform-specific bands were excised and DNA sequenced to confirm specificity.

Plasma sample analysis

Table 1 shows the m/z of the precursor and transition ions for surrogate peptides and internal standards. In all cases, we chose y-ions in high m/z ranges as transition ions to enhance the specificity and to minimize the interference from background.

Ideally, the calibration standards are prepared in the same biological matrix that is used for sample analysis. However, endogenous levels of OPN in plasma will affect the linearity of the concentration curve when no or low levels of OPN peptides are added to plasma. For this reason, we created a calibration curve by adding different amounts of native peptides to the fixed amount of heavy peptides in the range of 0.05 to 10.0 molar ratios, and measured ratios of the peak areas by MRM–MS under the same conditions used for plasma sample analysis. The concentration ratio versus peak area ratio was plotted. This approach circumvented the effect of endogenous peptides on the linearity of the calibration. The calibration curve for OPNc is shown in Figure 5. In our ion trap instrument, we estimate the range of linear detection is about 2 orders of magnitude. The range of linear detection could be further improved by using triple quadrupole type of the MS instruments (Kiernan et al. 2011, Kuhn et al. 2009, Nicol et al. 2008, Ocana & Neubert 2010).

We assessed the recovery of the protein by spiking in 1 ng, 2 ng, and 5 ng of the recombinant OPNa to a 0.1 mL of plasma sample which has very low endogenous OPNa, followed by the immunoaffinity capture and MRM–MS analysis of the OPNa peptide. Recovery for three spike-in experiments was 111.53 ± 1.3%, 78.8 ± 2.0% and 80.6 ± 5.9% respectively. Therefore, we estimate that our method has an approximately 80% accuracy rate for OPN quantification over a concentration range of 10-50 ng/ml. Due to the potential interference from the endogenous OPNa in plasma, recoveries at lower concentration ranges were not pursued.

Using the above described approach, we set out to determine the concentration of the various OPN slice variants in the plasma of 10 healthy individuals and 10 NSCLC patients. As shown in Figure 6, we observed a wide range of concentrations of the three isoforms in plasma. Mean concentrations of isoforms a, b, c in healthy individuals were 6.4, 1.5, and 0.4 ng/mL, respectively. In NSCLC patients, the mean concentration of OPNa was 29.5 ng/mL, significantly higher

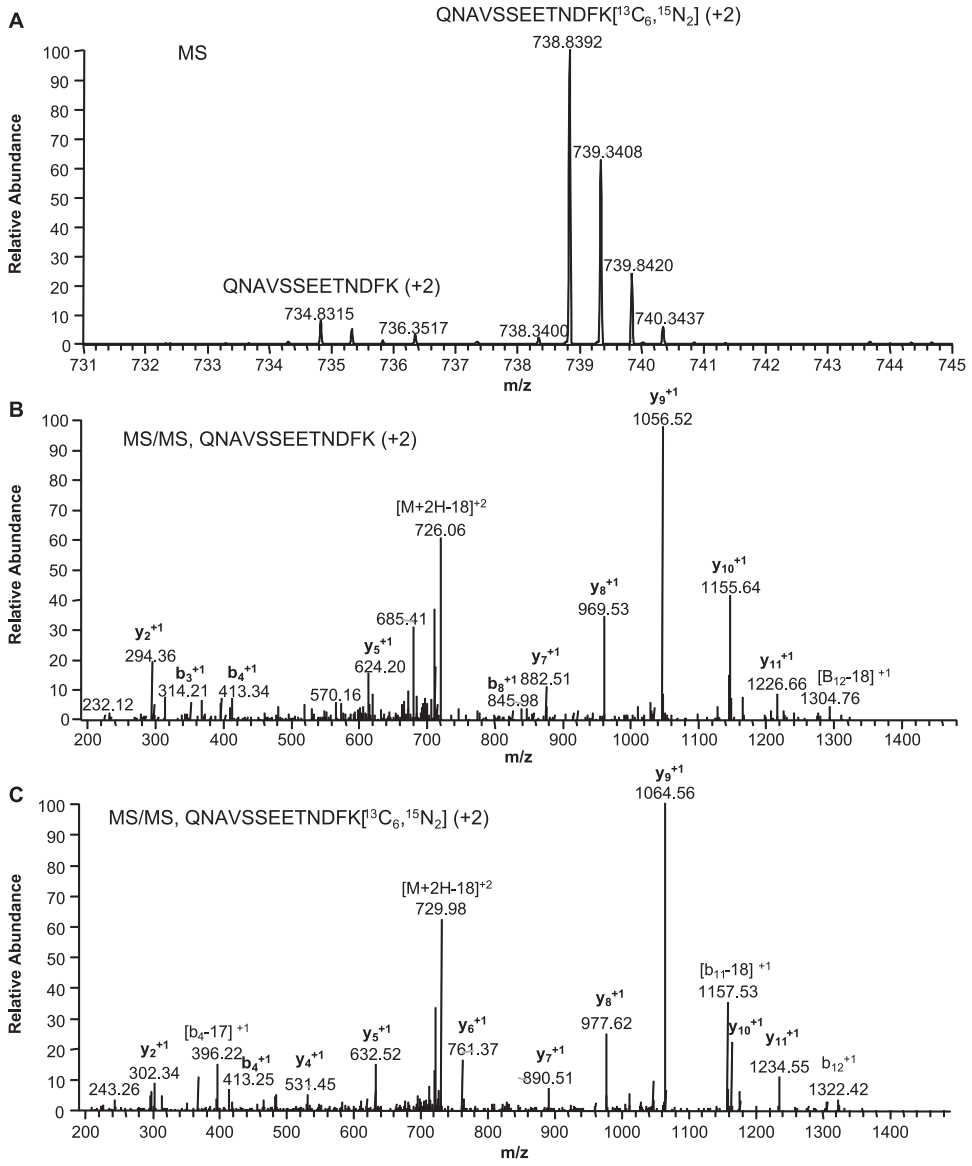

Figure 4. Identification of OPNc specific peptide in MDA-MB-435 conditioned medium. (A) Full scan MS of endogenous OPNc derived peptide and corresponding heavy labeled peptide. (B), MS/MS spectrum of the endogenous OPNc peptide, and (C) MS/MS spectrum of the heavy OPNc peptide.

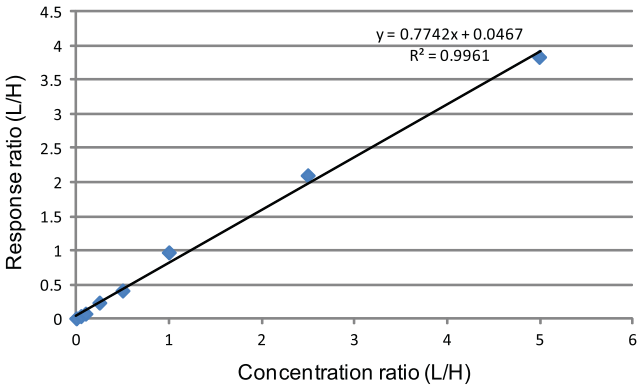

Figure 5. A plot of the ratio of native/heavy OPNc peptide verses the ratio of the peak areas measured by the MRM–MS.

than the mean concentration in healthy subjects. Interestingly, the OPNb and OPNc concentrations in patient sample NSCLC07 were dramatically higher than in other NSCLC patients. If this particular sample is excluded, the mean concentrations of the OPNb and OPNc in NSCLC plasma are 2.5 and 0.5 ng/mL respectively, which do not differ statistically from the mean concentration of the healthy plasma. Finally, the data presented here clearly demonstrate that overall OPN concentration, driven primarily by OPNa levels, is elevated in NSCLC plasma.

In order to cross validate our assay against more conventional ELISA methods we determined plasma OPNa levels using a solid phase ELISA kit from R&D systems using the provided calibrant. This kit was reported to be the most accurate among many commercially available ELISA kits (Plumer et al. 2008). Figure 7 shows a close correlation between the ELISA and MRM–MS assays. We therefore conclude that our method is a reliable approach for simultaneous quantification of all OPN splice variants in human plasma. Furthermore, our findings confirm elevation of

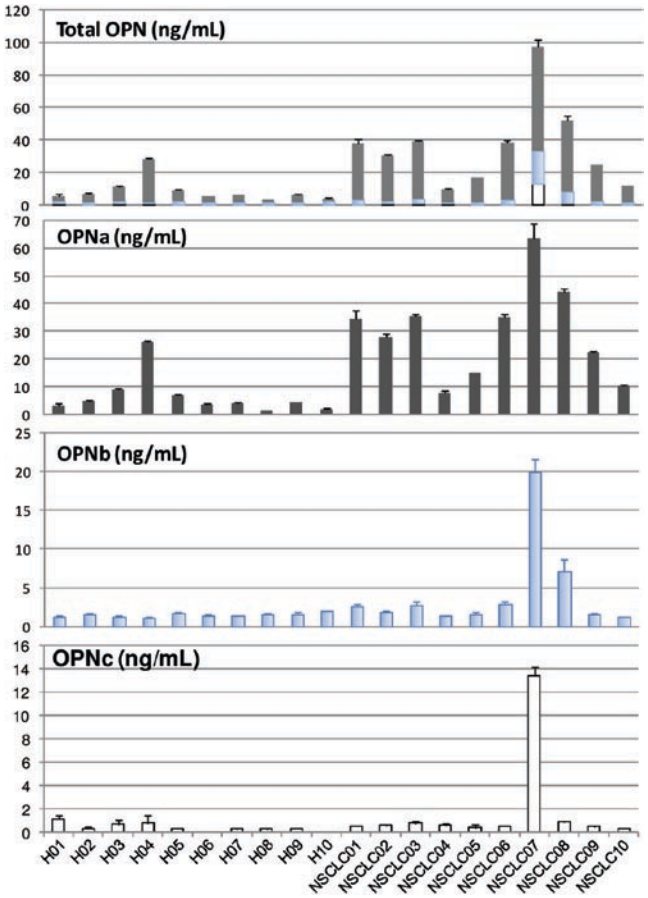

Figure 6. Plasma concentrations of OPN isoforms in healthy and NSCLC patients (as indicated) determined by immunoaffinity MRM–MS. In panel A total OPN concentration is shown along with the contribution of each isoform as indicated by their respective colors.

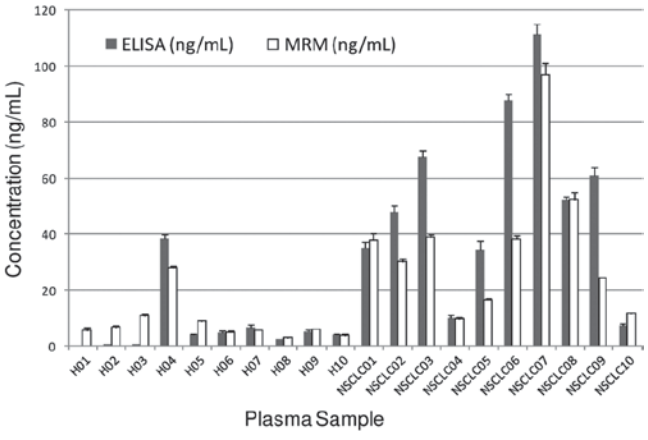

Figure 7. Correlation of OPN concentrations determined by ELISA and by MRM–MS method.

OPNa in cancer and also demonstrate that all three OPN isoforms are found in plasma from healthy subjects and are thus not specifically expressed in cancer patients.

Discussion

The existence of diverse forms of OPN resulting from alternative splicing and extensive post-translational modification has presented a major challenge to the investigators trying to understand OPN role in various diseases including cancer. It is likely that these individual isoforms may have distinct functional activities and can serve as diagnostic indicators of specific pathological events. However, the functional specificity and relative expression of individual OPN isoforms in tumor tissue and plasma are not well characterized. In most cases, researchers have assayed OPN isoforms in tumor tissue at the mRNA level, or measured plasma OPN concentrations by a traditional ELISA approach. A comprehensive understanding of the contribution of individual OPN splice variants to tumor progression would therefore require development of tool antibodies and analytical techniques that are capable of differentiating these highly similar isoforms.

Development of a highly specific immunoassay to measure different isoforms is challenging if not impossible. Selectivity offered by mass spectrometry is an attractive alternative approach. The primary objective of our investigation was to develop an MRM–MS based assay capable of simultaneously monitoring all OPN isoforms in plasma. A key to this approach was the selection of antibodies covering different sequence regions of OPN and therefore elimination of biases against any specific isoform. Extensively modified proteins, such as OPN, represent a significant challenge as most antibodies are raised using native peptide as an antigen and some are not suitable for immunoprecipitation. After judicious screening of various commercially available antibodies, we chose to use a combination of a large excess of O-17 polyclonal antibody (2 mg beads), together with three other antibodies recognizing various epitopes (0.5 mg beads each) for immunoaffinity capture. IP-Western experiments confirmed the combination was able to pull down all OPN from the plasma.

Immunoaffinity in conjunction with MRM–MS is primarily applied to the quantification of multiple biomarkers in plasma or serum, where one can always select the best surrogate peptides from an array of different peptides originating from an individual protein. Selection criteria for a surrogate peptide include (1) no reactive residues in the sequence, such as glutamine at the N-terminus, or Met, Trp, Cys residues, (2) complete cleavage at both sites, (3) no potential modifications such as glycosylation or phosphorylation, and (4) good peak shape in LC and high response in mass spectrometry. For OPN, unfortunately, following trypsin digestion, there was only one peptide unique to each isoform. Initial studies using cell conditioned medium indicated that some of the isoform-specific target peptides are partially phosphorylated and have missed trypsin cleavage at the C-terminal site, resulting in inconsistent and lower concentration readout. Initial efforts to improve digestion efficiency by increasing the trypsin/protein ratio, prolonged incubation, or use of Lys-C instead of trypsin, were not successful. We found that

the use of immobilized trypsin significantly promoted efficient digestion, leading to quantitative generation of the target peptides. Dephosphorylation of the tryptic peptides was effectively achieved by phosphatase treatment. During sample processing, conversion of glutamine to pyroglutamic acid was not observed. The MRM transition ion pairs listed in Table 1 were chosen for quantification not only because of their high intensity but also because transitions from doubly charged precursor to higher m/z fragment ions gave the best signal to noise ratio. This led to the improvement in the sensitivity and specificity of the detection.

Alternative splicing of OPN has been described in mesothelioma, breast cancer, hepatocellular carcinoma, glioma, lung cancer, head and neck squamous cell carcinoma (HNSCC), and ovarian cancers (Allan et al. 2006, Blasberg et al. 2010a, Blasberg et al. 2010b, Chang et al. 2007, Ivanov et al. 2009, Mi et al. 2004, Mirza et al. 2008, Paleari et al. 2009, Sullivan et al. 2009, Tilli et al. 2011, Vordermark et al. 2006, Zhao et al. 2011). Specific expression of a particular splice variant could provide a unique therapeutic target or a specific biomarker. This was thought to be the case for OPNc when it was reported to be specifically expressed in tumor tissues of breast and ovarian cancers (Mirza et al. 2008, Tilli et al. 2011). Although we cannot rule out local over-expression of OPNc in NSCLC our study clearly shows that it can be detected in the plasma of healthy individuals and therefore, is not an exclusive marker found in tumor bearing individuals. While local over-expression of OPNc in NSCLC tumors remains a possibility our study also shows that this would not significantly contribute to endogenous OPNc levels found in normal individuals. Furthermore, any therapeutic strategy targeting OPNc inhibition would have to take endogenous expression levels into account.

The MRM–MS data presented here clearly showed that OPNa is elevated in NSCLC patient plasma, whereas OPNb and OPNc are not. Although we only analyzed the limited number of clinical samples, this conclusion supports previous reports showing elevation of OPNa mRNA in most NSCLC tumors (Goparaju et al. 2010, Jain et al. 2007).

In conclusion, we have developed an immunoaffinity-mass spectrometry technique to quantitatively measure OPN isoforms in human plasma and successfully applied it to characterization of OPN isoforms in plasma from NSCLC patients. This method can be further applied to quantitative profiling of OPN isoforms in patient plasma from other cancer types in order to evaluate the potential use of individual OPN isoforms as biomarkers of specific cancers.

Declaration of interest

We certify that all authors have no financial or other conflict of interests in connection with the submitted article.

References

Allan AL, George R, Vantyghem SA, Lee MW, Hodgson NC, Engel CJ, Holliday RL, Girvan DP, Scott LA, Postenka CO, Al-Katib W, Stitt LW, Uede T, Chambers AF, Tuck AB. (2006). Role of the integrin-binding protein osteopontin in lymphatic metastasis of breast cancer. *Am J Pathol* 169:233–246.

Anborgh PH, Wilson SM, Tuck AB, Winquist E, Schmidt N, Hart R, Kon S, Maeda M, Uede T, Stitt LW, Chambers AF. (2009). New dual monoclonal ELISA for measuring plasma osteopontin as a biomarker associated with survival in prostate cancer: clinical validation and comparison of multiple ELISAs. *Clin Chem* 55:895–903.

Banerjee A, Lee JH, Ramaiah SK. (2008). Interaction of osteopontin with neutrophil α(4)β(1) and α(9)β(1) integrins in a rodent model of alcoholic liver disease. *Toxicol Appl Pharmacol* 233:238–246.

Blasberg JD, Goparaju CM, Pass HI, Donington JS. (2010a) Lung cancer osteopontin isoforms exhibit angiogenic functional heterogeneity. *J Thorac Cardiovasc Surg* 139:1587–1593.

Blasberg JD, Pass HI, Goparaju CM, Flores RM, Lee S, Donington JS. (2010b) Reduction of elevated plasma osteopontin levels with resection of non-small-cell lung cancer. *J Clin Oncol* 28:936–941.

Chae S, Jun HO, Lee EG, Yang SJ, Lee DC, Jung JK, Park KC, Yeom YI, Kim KW. (2009). Osteopontin splice variants differentially modulate the migratory activity of hepatocellular carcinoma cell lines. *Int J Oncol* 35:1409–1416.

Chang YS, Kim HJ, Chang J, Ahn CM, Kim SK, Kim SK. (2007). Elevated circulating level of osteopontin is associated with advanced disease state of non-small cell lung cancer. *Lung Cancer* 57:373–380.

Christensen B, Kazanecki CC, Petersen TE, Rittling SR, Denhardt DT, Sørensen ES. (2007). Cell type-specific post-translational modifications of mouse osteopontin are associated with different adhesive properties. *J Biol Chem* 282:19463–19472.

Christensen B, Nielsen MS, Haselmann KF, Petersen TE, Sørensen ES. (2005). Post-translationally modified residues of native human osteopontin are located in clusters: identification of 36 phosphorylation and five O-glycosylation sites and their biological implications. *Biochem J* 390:285–292.

Christensen B, Petersen TE, Sørensen ES. (2008). Post-translational modification and proteolytic processing of urinary osteopontin. *Biochem J* 411:53–61.

Courter D, Cao H, Kwok S, Kong C, Banh A, Kuo P, Bouley DM, Vice C, Brustugun OT, Denko NC, Koong AC, Giaccia A, Le QT. (2010). The RGD domain of human osteopontin promotes tumor growth and metastasis through activation of survival pathways. *PLoS ONE* 5:e9633.

Creaney J, Yeoman D, Musk AW, de Klerk N, Skates SJ, Robinson BW. (2011). Plasma versus serum levels of osteopontin and mesothelin in patients with malignant mesothelioma–which is best? *Lung Cancer* 74:55–60.

Goparaju CM, Pass HI, Blasberg JD, Hirsch N, Donington JS. (2010). Functional heterogeneity of osteopontin isoforms in non-small cell lung cancer. *J Thorac Oncol* 5:1516–1523.

He B, Mirza M, Weber GF. (2006). An osteopontin splice variant induces anchorage independence in human breast cancer cells. *Oncogene* 25:2192–2202.

Ivanov SV, Ivanova AV, Goparaju CM, Chen Y, Beck A, Pass HI. (2009). Tumorigenic properties of alternative osteopontin isoforms in mesothelioma. *Biochem Biophys Res Commun* 382:514–518.

Jain S, Chakraborty G, Bulbule A, Kaur R, Kundu GC. (2007). Osteopontin: an emerging therapeutic target for anticancer therapy. *Expert Opin Ther Targets* 11:81–90.

Kazanecki CC, Uzwiak DJ, Denhardt DT. (2007). Control of osteopontin signaling and function by post-translational phosphorylation and protein folding. *J Cell Biochem* 102:912–924.

Keykhosravani M, Doherty-Kirby A, Zhang C, Brewer D, Goldberg HA, Hunter GK, Lajoie G. (2005). Comprehensive identification of post-translational modifications of rat bone osteopontin by mass spectrometry. *Biochemistry* 44:6990–7003.

Kiernan UA, Phillips DA, Trenchevska O, Nedelkov D. (2011). Quantitative mass spectrometry evaluation of human retinol binding protein 4 and related variants. *PLoS ONE* 6:e17282.

Kuhn E, Addona T, Keshishian H, Burgess M, Mani DR, Lee RT, Sabatine MS, Gerszten RE, Carr SA. (2009). Developing multiplexed assays for troponin I and interleukin-33 in plasma by peptide immunoaffinity enrichment and targeted mass spectrometry. *Clin Chem* 55:1108–1117.

Kuhn E, Wu J, Karl J, Liao H, Zolg W, Guild B. (2004). Quantification of C-reactive protein in the serum of patients with rheumatoid arthritis using multiple reaction monitoring mass spectrometry and 13C-labeled peptide standards. *Proteomics* 4:1175–1186.

Mack PC, Redman MW, Chansky K, Williamson SK, Farneth NC, Lara PN Jr, Franklin WA, Le QT, Crowley JJ, Gandara DR; SWOG. (2008). Lower osteopontin plasma levels are associated with superior outcomes in advanced non-small-cell lung cancer patients receiving platinum-based chemotherapy: SWOG Study S0003. *J Clin Oncol* 26:4771–4776.

Makawita S, Diamandis EP. (2010). The bottleneck in the cancer biomarker pipeline and protein quantification through mass spectrometry-based approaches: current strategies for candidate verification. *Clin Chem* 56:212–222.

Meng Z, Veenstra TD. (2011) Targeted mass spectrometry approaches for protein biomarker verification. *J Proteomics* 74:2650.

Mi Z, Guo H, Wai PY, Gao C, Wei J, Kuo PC. (2004). Differential osteopontin expression in phenotypically distinct subclones of murine breast cancer cells mediates metastatic behavior. *J Biol Chem* 279:46659–46667.

Mirza M, Shaughnessy E, Hurley JK, Vanpatten KA, Pestano GA, He B, Weber GF. (2008). Osteopontin-c is a selective marker of breast cancer. *Int J Cancer* 122:889–897.

Nicol GR, Han M, Kim J, Birse CE, Brand E, Nguyen A, Mesri M, FitzHugh W, Kaminker P, Moore PA, Ruben SM, He T. (2008). Use of an immunoaffinity-mass spectrometry-based approach for the quantification of protein biomarkers from serum samples of lung cancer patients. *Mol Cell Proteomics* 7:1974–1982.

Ocaña MF, Neubert H. (2010). An immunoaffinity liquid chromatography-tandem mass spectrometry assay for the quantitation of matrix metalloproteinase 9 in mouse serum. *Anal Biochem* 399:202–210.

Paleari L, Rotolo N, Imperatori A, Puzone R, Sessa F, Franzi F, Meacci E, Camplese P, Cesario A, Paganuzzi M. (2009). Osteopontin is not a specific marker in malignant pleural mesothelioma. *Int J Biol Markers* 24:112–117.

Plumer A, Duan H, Subramaniam S, Lucas FL, Miesfeldt S, Ng AK, Liaw L. (2008). Development of fragment-specific osteopontin antibodies and ELISA for quantification in human metastatic breast cancer. *BMC Cancer* 8:38.

Rangaswami H, Bulbule A, Kundu GC. (2006). Osteopontin: role in cell signaling and cancer progression. *Trends Cell Biol* 16:79–87.

Shakey Q, Bates B, Wu J. (2010). An approach to quantifying N-linked glycoproteins by enzyme-catalyzed 18O3-labeling of solid-phase enriched glycopeptides. *Anal Chem* 82:7722–7728.

Sullivan J, Blair L, Alnajar A, Aziz T, Ng CY, Chipitsyna G, Gong Q, Witkiewicz A, Weber GF, Denhardt DT, Yeo CJ, Arafat HA. (2009). Expression of a prometastatic splice variant of osteopontin, OPNC, in human pancreatic ductal adenocarcinoma. *Surgery* 146:232–240.

Tilli TM, Franco VF, Robbs BK, Wanderley JL, da Silva FR, de Mello KD, Viola JP, Weber GF, Gimba ER. (2011). Osteopontin-c splicing isoform contributes to ovarian cancer progression. *Mol Cancer Res* 9:280–293.

Vordermark D, Said HM, Katzer A, Kuhnt T, Hänsgen G, Dunst J, Flentje M, Bache M. (2006). Plasma osteopontin levels in patients with head and neck cancer and cervix cancer are critically dependent on the choice of ELISA system. *BMC Cancer* 6:207.

Wai PY, Kuo PC. (2008). Osteopontin: regulation in tumor metastasis. *Cancer Metastasis Rev* 27:103–118.

Weber GF, Zawaideh S, Hikita S, Kumar VA, Cantor H, Ashkar S. (2002). Phosphorylation-dependent interaction of osteopontin with its receptors regulates macrophage migration and activation. *J Leukoc Biol* 72:752–761.

Zhao B, Sun T, Meng F, Qu A, Li C, Shen H, Jin Y, Li W. (2011). Osteopontin as a potential biomarker of proliferation and invasiveness for lung cancer. *J Cancer Res Clin Oncol* 137:1061–1070.